

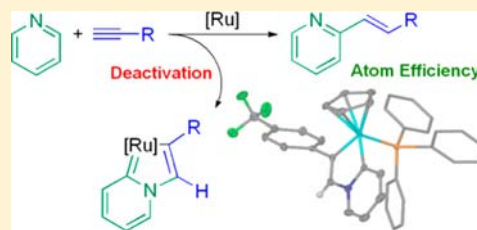
Ruthenium-Mediated C–H Functionalization of Pyridine: The Role of Vinylidene and Pyridylidene Ligands

David G. Johnson, Jason M. Lynam,* Neetisha S. Mistry, John M. Slattery,* Robert J. Thatcher, and Adrian C. Whitwood

Department of Chemistry, University of York, Heslington, York, YO10 5DD, U.K.

S Supporting Information

ABSTRACT: A combined experimental and theoretical study has demonstrated that $[\text{Ru}(\eta^5\text{-C}_5\text{H}_5)(\text{py})_2(\text{PPh}_3)]^+$ is a key intermediate, and active catalyst for, the formation of 2-substituted *E*-styrylpyridines from pyridine and terminal alkynes $\text{HC}\equiv\text{CR}$ ($\text{R} = \text{Ph}, \text{C}_6\text{H}_4\text{-4-CF}_3$) in a 100% atom efficient manner under mild conditions. A catalyst deactivation pathway involving formation of the pyridylidene-containing complex $[\text{Ru}(\eta^5\text{-C}_5\text{H}_5)(\kappa^3\text{-C}_3\text{H}_4\text{NCH}=\text{CHR})(\text{PPh}_3)]^+$ and subsequently a 1-ruthenaindolizine complex has been identified. Mechanistic studies using ^{13}C - and D -labeling and DFT calculations suggest that a vinylidene-containing intermediate $[\text{Ru}(\eta^5\text{-C}_5\text{H}_5)(\text{py})(=\text{C}=\text{CHR})(\text{PPh}_3)]^+$ is formed, which can then proceed to the pyridylidene-containing deactivation product or the desired product depending on the reaction conditions. Nucleophilic attack by free pyridine at the α -carbon in this complex subsequently leads to formation of a C–H agostic complex that is the branching point for the productive and unproductive pathways. The formation of the desired products relies on C–H bond cleavage from this agostic complex in the presence of free pyridine to give the pyridyl complex $[\text{Ru}(\eta^5\text{-C}_5\text{H}_5)(\text{C}_5\text{H}_4\text{N})(=\text{C}=\text{CHR})(\text{PPh}_3)]$. Migration of the pyridyl ligand (or its pyridylidene tautomer) to the α -carbon of the vinylidene, followed by protonation, results in the formation of the 2-styrylpyridine. These studies demonstrate that pyridylidene ligands play an important role in both the productive and nonproductive pathways in this catalyst system.

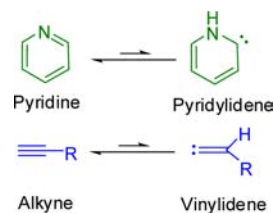


INTRODUCTION

The selective, direct C–H functionalization of organic substrates by transition metal compounds is an attractive method for structural elaboration.¹ By circumventing the use of halogenated substrates in metal-catalyzed reactions (which are often prepared from the parent hydrocarbon) salt-based byproducts are eliminated thus greatly improving atom-efficiency and facilitating isolation of the product.² Direct C–H functionalization has been achieved by a number of methods. One popular strategy is to employ a directing group, such as a heteroatom or unsaturated tether, to dictate coordination to the metal.³ The C–H activation event may also be aided by the presence of an intramolecular base, such as a carboxylate or carbonate ligand, which facilitates the deprotonation of the substrate.⁴ The formation of a (cyclo)metalated substrate then allows for the key carbon–carbon bond formation, either via electrophilic or oxidative coupling.^{3g}

An alternative pathway to activate heterocyclic substrates is to exploit the reactivity of their carbene-containing tautomers.⁵ As shown below, pyridylidene is a high energy tautomer of pyridine, in which a formal hydrogen migration has occurred to reveal an unsaturated carbene.⁶ This may be viewed as being similar to the well-established alkyne/vinylidene tautomerization.⁷ Transition metal complexes may facilitate the formation of pyridylidene groups from pyridine derivatives, in a similar fashion to that for alkynes and vinylidenes. There are a number of examples of metal centers which are able to promote the

conversion of heterocyclic substrates to their N-heterocyclic carbene forms. For example, the reaction of iridium complexes containing *tris*-pyrazolylborate ligands with 2-substituted pyridine derivatives may result in the formation of pyridylidene ligands.⁸ Although the established tendency of the *tris*-pyrazolylborate iridium fragment to support carbene ligands is an important factor in assisting this process, the relief of steric strain by removing the substituent in the 2-position away from the local coordination sphere of the metal also acts as a driving force. Again, a similar steric driving force is often invoked for the formation of vinylidene ligands from the corresponding alkyne complex. The number of examples in which unsubstituted pyridine may be transformed to the parent pyridylidene is limited.^{8b}



An alternative strategy to stabilize the pyridylidene tautomer of both substituted pyridines and quinolines has focused on

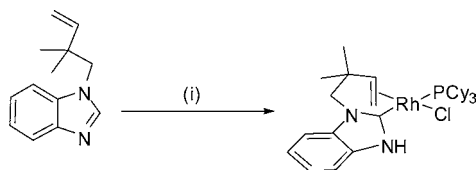
Received: October 2, 2012

Published: December 17, 2012

exploiting hydrogen bonding between the resulting N–H group and a halide ligand within the coordination sphere of Group 8 and 9 metals.⁹ Other examples based on the transformation of imidazole ligands to N-heterocyclic carbenes promoted by molybdenum,¹⁰ manganese,¹¹ and rhenium¹² have also been reported. The reverse process, conversion of an N-heterocyclic carbene to a substituted imidazole, has also been observed.¹³

As is also the case with alkyne and vinylidene ligands,¹⁴ the formation of the carbene tautomer involves a C–H bond activation and it might be expected that the carbene form will display markedly different reactivity from the parent heterocycle. However, the number of examples where parent pyridylidenes have been implicated in the mechanism of stoichiometric or catalytic functionalization of heterocycles is limited.¹⁵ Therefore the possibility exists for utilizing this tautomerization in a synthetically useful manner to activate nitrogen-containing heterocycles.

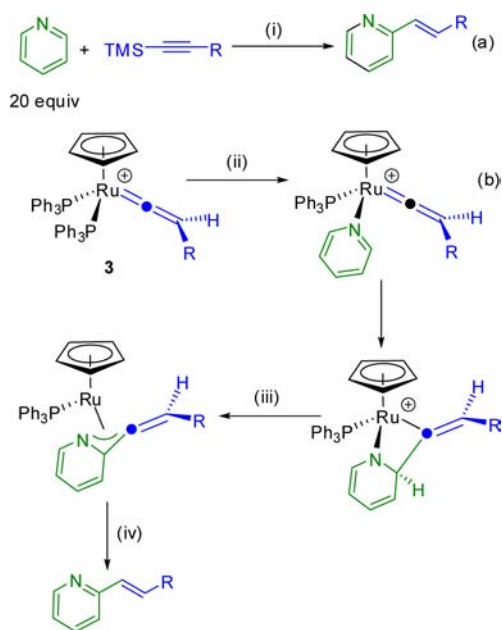
An analogy may be drawn between the work of Bergman and Ellman, for the direct functionalization of heterocyclic substrates.¹⁶ It has been established that the key step in this process is the rhodium-mediated conversion of a heterocycle into its N-heterocyclic carbene tautomer (Scheme 1).¹⁷ The

Scheme 1^a

^a(i) [RhCl(coe)₂]₂, PCy₃, 75 °C, 3 h, THF.

formation of the carbene complex activates the heterocycle and subsequent coupling between the metal-bound carbon atoms and unsaturated substrates, as well as aromatic halides has been achieved. The demonstration that pyridylidene ligands offer potential routes to the direct functionalization of pyridine and related heterocycles is therefore of clear importance.

In 2003, Murakami and Hori demonstrated that a system based on [Ru(η^5 -C₅H₅)Cl(PPh₃)₂], **1**, and NaPF₆ was able to catalyze the formation of 2-styrylpyridine from pyridine (which acts as both substrate and solvent) and a trimethylsilyl-protected alkyne (Scheme 2a).¹⁸ The reaction selectivity resulted in substitution at the 2-position of pyridine and only the *E*-isomer of the alkene was obtained. It was proposed that vinylidene complexes (which may be obtained by reaction of **1** with terminal alkynes HC≡CR, **2**, in the presence of a halide scavenger) [Ru(η^5 -C₅H₅)(=C=CHR)(PPh₃)₂]⁺, [**3**]⁺, were intermediates in this process. An intramolecular coupling between coordinated pyridine and the vinylidene was proposed as the key step in the formation of the product (Scheme 2b). This reaction has some extremely attractive features, notably it is a relatively atom-efficient method to prepare functionalized pyridines. However, the high ruthenium catalyst loading (20 mol %), reaction temperature (150 °C) and the necessity of using silyl-protected alkynes, are significant drawbacks. This prompted us to employ a mechanism-driven approach, using a combination of experimental and theoretical studies, to gain insight into the fundamental processes controlling both C–H activation of the pyridine and the subsequent C–C bond formation.

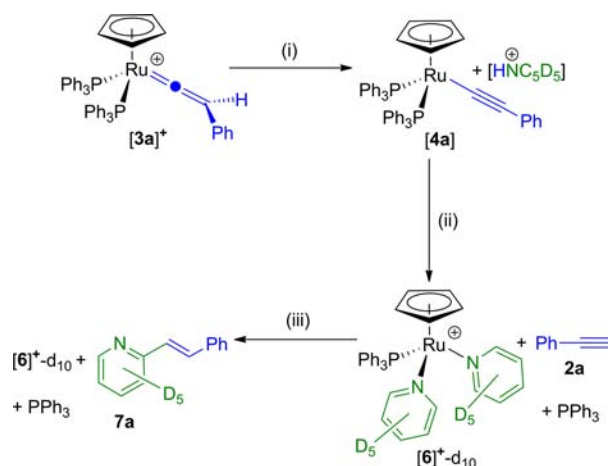
Scheme 2^a

^a(a)(i) + 20 mol % **1**, 22 mol % NaPF₆, 150 °C, 7 h; (b) mechanism proposed by Murakami and Hori for the formation of 2-styrylpyridine.¹⁸ (ii) +py, –PPh₃; (iii) +py, –[Hpy]⁺; (iv) +[Hpy]⁺, –py.

We now report that [Ru(η^5 -C₅H₅)(py)₂(PPh₃)₂]⁺ is able to promote the formation of 2-styrylpyridine derivatives under mild conditions via direct coupling of terminal alkynes with pyridine. A deactivation pathway involving the formation of a pyridylidene ligand has been identified, as have the key C–H cleavage and C–C bond formation steps. The latter involves the migration of a pyridyl (or pyridylidene ligand) to the metal-bound carbon atom of a vinylidene ligand. Thus, we propose that pyridylidene ligands play an important role in both the productive and nonproductive pathways for this catalyst system.

RESULTS AND DISCUSSION

Experimental Studies. Initial studies of the isotopically enriched complex [Ru(η^5 -C₅H₅)(=C¹³C=CHPh)(PPh₃)₂]⁺, [**3a**]⁺-¹³C found that dissolution of deep-red [**3a**]⁺-¹³C in d₅-pyridine resulted in the rapid formation of a yellow solution. A ¹³C{¹H} NMR spectrum of this solution showed that the vinylidene complex (typical $\delta_{Ca} \approx 350$)^{7a} had been deprotonated by pyridine to give the alkynyl complex [Ru(η^5 -C₅H₅)(-C¹³C≡CPh)(PPh₃)₂]⁺, [**4a**]⁺-¹³C (δ_{Ca} 117.7 (²J_{PC} = 24.8 Hz, identified by comparison to an authentic sample of [**4a**]) (Scheme 3).¹⁹ As the reported conditions for catalysis occurred at elevated temperature, the reaction mixture was heated to 125 °C. After 1 h, the resonances for [**4a**]⁺-¹³C in the ¹³C{¹H} and ³¹P{¹H} NMR spectra had decreased in intensity and signals due to H¹³C≡CPh and uncoordinated PPh₃ were observed, along with a new singlet resonance at δ_p 48.7 (approximately a 1:1 ratio with free PPh₃). In some instances a small quantity of OPPh₃ and [Ru(η^5 -C₅H₅)(¹³CO)(PPh₃)₂]⁺, [**5**]⁺-¹³C were also generated in these reactions, the latter presumably arising from either hydrolysis or oxidation of the vinylidene ligand.²⁰ After the mixture was heated for 23 h the ratio of [**4a**]⁺-¹³C to the species with the resonance at δ_p 48.7

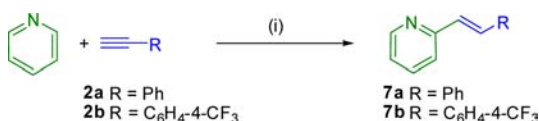
Scheme 3^a

^a(i) d₅-pyridine, room temperature; (ii) 120 °C, 1 h; (iii) 120 °C, 23 h.

was ~1:3 and any free H¹³C≡CPh had been converted to *E*-2-styrylpyridine **7a**.

These data indicated that on heating a new ruthenium species containing a single PPh₃ ligands, in which the alkyne was no longer coordinated to the metal, had been formed. We speculated that the vinylidene and a PPh₃ ligand may have been replaced by the solvent, d₅-pyridine, to give [Ru(η⁵-C₅H₅)(d₅-py)₂(PPh₃)]⁺, [6]⁺-d₁₀. Complex [6]PF₆ was prepared independently by reaction of [Ru(η⁵-C₅H₅)(NCMe)₂(PPh₃)]-[PF₆], **8**[PF₆],²¹ with an excess of pyridine and its NMR spectra were identical to those observed on heating [3a]PF₆.

Treatment of [6]PF₆ with an equimolar amount of either HC≡CPh, **2a**, or HC≡C-C₆H₄-4-CF₃, **2b**, in pyridine solution followed by heating at 50 °C for 24 h resulted in the quantitative formation of *E*-2-styrylpyridines, **7a** and **7b** respectively (Scheme 4). The ³¹P{¹H} NMR spectrum of the

Scheme 4^a

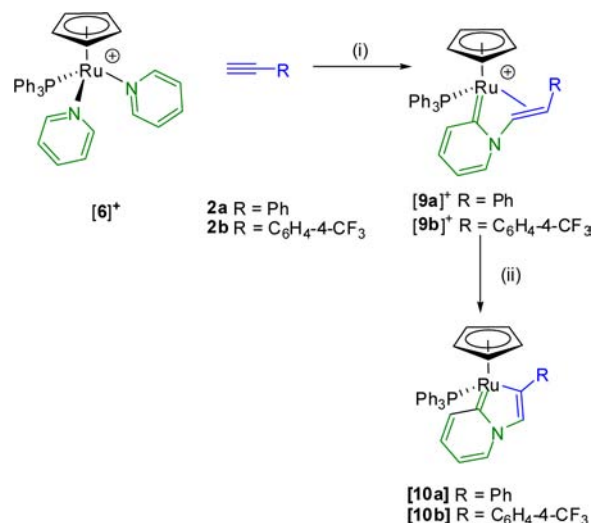
^a(i) + [6]PF₆, 50 °C, 24 h.

crude reaction mixture recorded in d₅-pyridine solution demonstrated that [6]PF₆ was still the major phosphorus-containing compound in the reaction mixture. Further stoichiometric aliquots of the alkyne could be added to this solution, which, after heating, resulted in the formation of additional **7**. However, during the course of these procedures a new resonance at δ_p 61.6 was observed to increase in intensity in the ³¹P{¹H} NMR spectra, and a corresponding resonance in the cyclopentadienyl region of the ¹H NMR spectrum was observed at δ_H 5.00, indicating the formation of a new ruthenium species.

The reaction was attempted with a substoichiometric amount of [6]PF₆ but at a significantly lower temperature than that employed by Murakami and Hori. Heating complex [6]PF₆ (20 mol %) in pyridine solution with either **2a** or **2b** for 16 h at 50 °C resulted in the formation of some of the desired product **7**, but only ~50% conversion was observed (based on conversion

of alkyne). The ³¹P{¹H} NMR spectrum demonstrated that significant quantities of the product that exhibited a resonance at δ_p 61.6 were present which, in the stoichiometric and substoichiometric reactions, appears to inhibit the formation of **7**. Repeating the reaction between [6]PF₆ and **2b** in pyridine but at 100 °C and using focused microwave radiation did result in the formation of some **7b**, however significant quantities of the head-to-tail alkyne dimer ArCH=CH-C≡CAr (Ar = C₆H₄-4-CF₃) were also formed.²² These data indicate that, by virtue of being able to perform the coupling reaction at a lower temperature, alkyne dimerization is inhibited when [6]PF₆ is employed as a catalyst. As it is unnecessary to employ trimethylsilyl-protected substrates, [6]PF₆ promotes the formation of **7** with 100% atom efficiency, albeit with 50% conversion.

Solvent Dependence. The reaction between [6]PF₆ and either **2a** or **2b** exhibited a marked solvent dependence. In contrast to the results obtained in pyridine solution, treatment of a CH₂Cl₂ solution of [6]PF₆ with either **2a** or **2b** did not result in the formation of the desired products **7a** or **7b**. After heating at 50 °C for 15 h the major organometallic product from the reactions were shown to be [9a]⁺ and [9b]⁺ (Scheme 5). The structures of both complexes were established by single

Scheme 5^a

^a(i) CH₂Cl₂ 50 °C, 15 h. (ii) py or +DABCO, -[HDABCO]PF₆, CH₂Cl₂.

crystal X-ray diffraction ([9a]⁺ Figure 1, [9b]⁺ Supporting Information) and the resulting structural determinations demonstrated that an unusual coupling reaction between the alkyne and pyridine had occurred to give a substituted pyridylidene ligand in which the N-heterocyclic carbene ligand is tethered to the metal by a pendant alkene.

The formulation for complexes [9a]⁺ and [9b]⁺ is supported by NMR spectroscopy. Using [9b]⁺ as an example, the ¹³C{¹H} NMR spectrum exhibited a doublet resonance for the metal-bound carbon atom at δ_C 179.6 (²J_{PC} = 19.1 Hz), consistent with the presence of the N-heterocyclic carbene ligand. A doublet resonance at δ_C 66.6 (²J_{PC} = 3.5 Hz) and a singlet at δ_C 54.8 were assigned to the two carbon atoms of the coordinated-alkene group. As shown by a 2D-HMQC experiment, these two resonances were attached to hydrogen atoms exhibiting peaks at δ_H 3.60 (dd, 1H, ³J_{HP} = 11.4 Hz, ³J_{HH} = 7.9 Hz) and δ_H 6.77

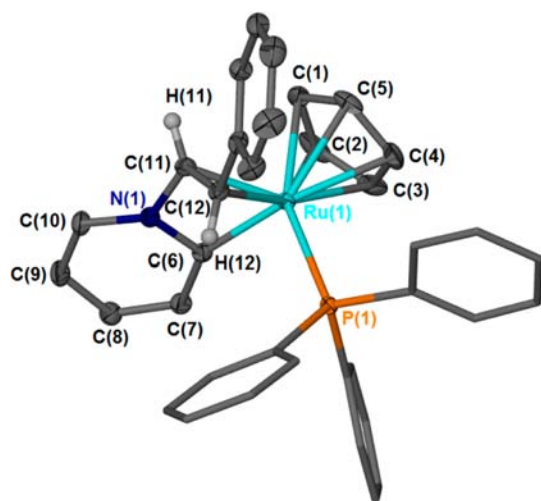


Figure 1. Solid-state structure of the cation $[9a]^+$. Thermal ellipsoids (where shown) at the 50% probability level, hydrogen atoms (except H(11) and H(12)) omitted for clarity.

(d, $1H$, $^3J_{HH} = 7.9$ Hz) respectively. A 1H - 1H COSY experiment demonstrated that these two alkene peaks were mutually coupled and a 1H - 1H NOESY spectrum illustrated that the proton responsible for the resonance at δ_H 6.77 was orientated toward the cyclopentadienyl ligand, hence this resonance was assigned to H(11) (Figure 1): the peak at δ_H 3.60 was attributed to H(12). The 1H NMR spectrum of both $[9a]PF_6$ and $[9b]PF_6$ were temperature dependent. At room temperature only broad resonances were observed for the aromatic groups of the PPh_3 ligand. At 220 K separate peaks for each of the three phenyl groups of the phosphine ligand were observed, consistent with rotation of the PPh_3 group being restricted on the NMR time scale.²³

Dissolution of an isolated sample of bright yellow $[9b]PF_6$ in d_5 -pyridine resulted in the formation of a red solution which exhibited a single resonance in the $^{31}P\{^1H\}$ NMR spectrum at δ_p 61.6. The 1H NMR spectrum exhibited a broad resonance at δ_H 17.4 which was assigned as a pyridinium ion N-H proton. It was concluded that the pyridine solvent had acted to deprotonate the organic ligand bound to ruthenium to give a new species $[10b]$ (Scheme 5).

Complex $[10b]$ could also be prepared from the reaction of $[9b]^+$ with DABCO in CH_2Cl_2 solution. After removal of the solvent, the product was extracted with pentane and cooling the resulting solution to -20 °C afforded crystals of $[10b]$ suitable for study by single crystal X-ray diffraction (Figure 2a). The subsequent structural determination demonstrated that $[9b]^+$ had been deprotonated to produce a complex which is probably best viewed as containing a 1-ruthanaindolizine ligand, similar to the 3-osmaindolizine and 3-ruthanaindolizine complexes obtained from the deprotonation of complexes containing N-bound 2-vinylpyridine ligands.²⁴ The bond lengths within the metallaindolizine rings in $[10b]$ (Figure 2b) and its $^{13}C\{^1H\}$ NMR spectrum (δ_C 219.3 [C(6)] and δ_C 190.2 [C(12)]) suggest that the structure is probably best described by a pyridylidene-vinyl resonance form.

The metrical parameters from the molecular structures of complexes $[9a]^+$, $[9b]^+$, and $[10b]$ are consistent with a contribution from a ruthenium pyridylidene resonance form. The ruthenium-carbon bonds in $[9a]^+$ and $[9b]^+$ (2.039(2) Å $[9a]^+$, 2.029(3) Å $[9b]^+$) are shorter than those observed in

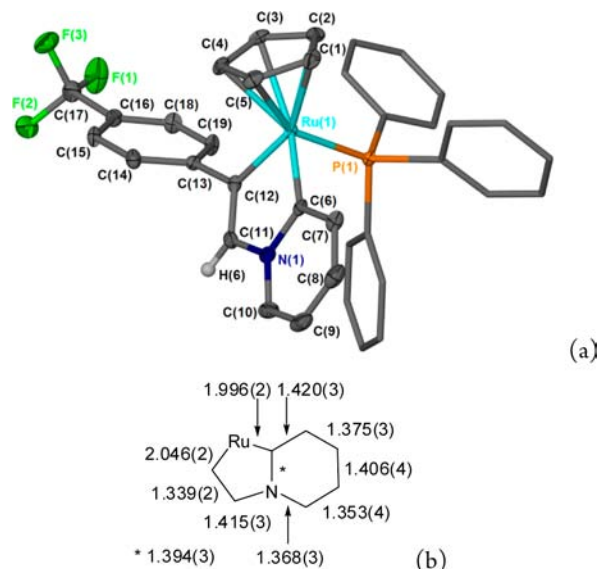


Figure 2. (a) Solid-state structure of the $[10b]$. Thermal ellipsoids (where shown) are at the 50% probability level and hydrogen atoms (except H(11)) and the pentane of crystallization were omitted for clarity. (b) Bond lengths (Å) within the 1-ruthanaindolizine group.

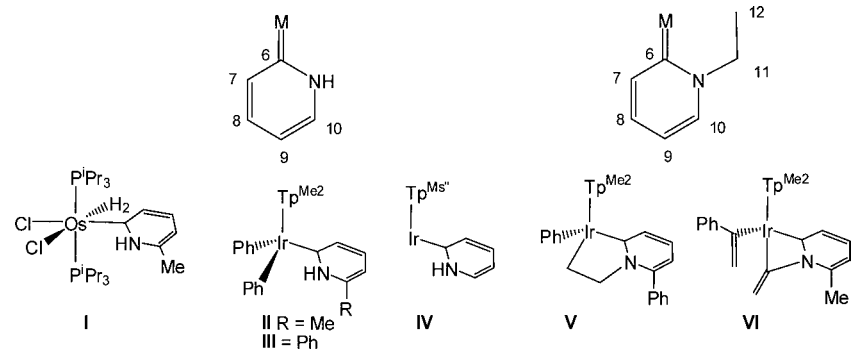
related phenyl-containing ruthenium half-sandwich compounds, where the metal-carbon bonds typically fall within the region 2.06–2.10 Å.²⁵ NBO analysis (see Supporting Information) of the DFT-optimized cation $[9a]^+$ also suggests significant pyridylidene character. Although the NBO reference structure for this ion contains a Ru-C single bond and C(6)-N(1) double bond, there is significant donation of metal-based electron density to the C-N π^* orbital (occupation = 0.478 e^- ; total second order perturbation stabilization energy for these interactions = 63 kJ mol^{-1}) giving some π -character to the M-C bond. This is very similar to bonding in the pyridylidene complex $[P]^+$ (Scheme 11), but quite different from the related pyridyl complex $[O]$ (Scheme 11) (C-N π^* occupation = 0.362 e^- , total second order perturbation stabilization energy = 34 kJ mol^{-1}). The Ru-C(6) bond length in $[10b]$ is shorter than those in $[9]^+$ and a lower field chemical shift of C(6) is observed. Similarly to the experimental data, NBO analysis of $[10a]$ suggests a more localized bonding regime in the C_5N ring {Wiberg bond indices (WBI) for C(7)-C(8) and C(9)-C(10) are 1.569 and 1.618 respectively} compared to $[9a]^+$ (WBI = 1.490 and 1.513) with significant π character to the M=C bond.

A comparison of the bond lengths and $^{13}C\{^1H\}$ NMR data for $[9a]^+$, $[9b]^+$ and $[10b]$ with Ir and Os complexes containing pyridylidene ligands that have been reported in the literature is presented in Table 1. The data indicates that for the iridium complexes the metal-carbon bonds are generally shorter than in $[9]^+$ and closer to those observed in $[10b]$. This may indicate greater pyridylidene character in these cases when compared to $[9]^+$ and the osmium species I.

NMR spectra of crystals of $[10b]$ in d_5 -pyridine solution contained resonances that were identical to the product observed in the reactions between $[6]PF_6$ and **2b** in pyridine solution, whose presence coincided with a decrease in activity.

Heating a sample of $[10b]$ in d_5 -pyridine solution in the presence of $[Hpy]PF_6$ did not exhibit any significant changes until 150 °C, when new resonances were observed that were identical to **7b**. In contrast, heating $[10b]$ in the absence of

Table 1. Bond lengths (Å) and chemical shifts for selected complexes containing pyridylidene ligands. Tp^{Me_2} = hydrotris(3,5-dimethylpyrazolyl)borate, TpMs'' = dimetaltedhydrotris(3,5-dimesitylpyrazolyl)borate



	[9a] ⁺	[9b] ⁺	[10b]	I ^{9d}	II ^{8a}	III ^{8a}	IV ^{8b}	V ^{8d}	VI ^{8d}
M–C(6)	2.039(2)	2.029(3)	1.996(2)	2.055(8)	1.982(2)	1.978(3)	1.975(2)	1.949(3)	1.97(2)
C(6)–N(1)	1.359(2)	1.360(3)	1.394(3)	1.366(9)	1.366(3)	1.369(4)	1.368(3)	1.384(4)	1.42(2)
C(6)–C(7)	1.406(3)	1.401(4)	1.420(3)	1.41(1)	1.422(2)	1.431(4)	1.423(4)	1.414(4)	1.40(2)
C(7)–C(8)	1.388(3)	1.380(4)	1.375(3)	1.37(1)	1.373(3)	1.379(4)	1.369(4)	1.369(5)	1.52(3)
C(8)–C(9)	1.402(3)	1.405(4)	1.406(4)	1.39(1)	1.402(3)	1.397(6)	1.402(3)	1.402(6)	1.59(3)
C(9)–C(10)	1.373(3)	1.367(4)	1.353(4)	1.35(1)	1.358(3)	1.366(5)	1.363(4)	1.371(5)	1.38(2)
C(10)–N(1)	1.349(2)	1.353(3)	1.368(3)	1.39(1)	1.364(2)	1.396(5)	1.361(4)	1.375(4)	1.36(2)
N(1)–C(11)	1.453(2)	1.459(3)	1.415(3)					1.500(4)	1.43(2)
C(11)–C(12)	1.405(3)	1.411(4)	1.339(3)					1.533(4)	1.31(2)
M–C(11)	2.152(2)	2.127(3)	2.046(2)						2.02(1)
M–C(12)	2.258(2)	2.245(3)						2.063(3)	
$\delta^{13}\text{C}$ C(6)		179.6	219.3	182.6		171.9	183.1	190.6	160.9

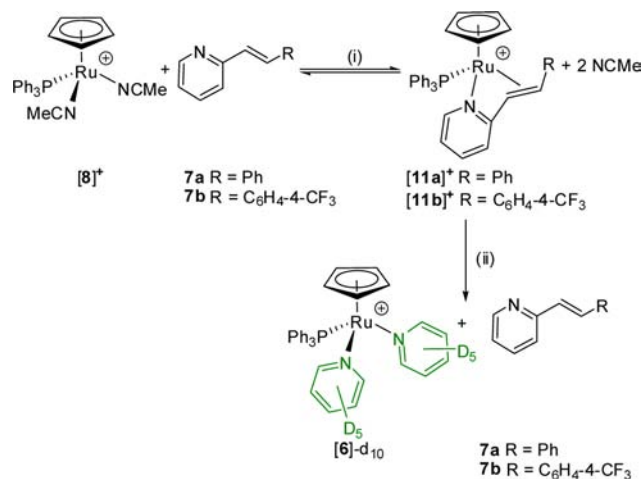
[Hpy]⁺ did not result in the formation of the organic product. The conditions required to form **7b** from **[10b]** are far more forcing than those observed in the reactions promoted by **[6]⁺** indicating that the formation of **[10]** represents a catalyst deactivation process and is generated in a process which is competitive to that which yields **7**.

The synthesis of complexes containing N-bound 2-styrylpyridine ligands was targeted to ensure that product coordination did not inhibit the subsequent regeneration of **[6]⁺**. Reaction of the acetonitrile complex **[8]PF₆** with either **7a** or **7b** resulted in the ultimate formation of complexes **[11a]⁺** and **[11b]⁺** respectively (Scheme 6). An NMR study of the

reaction revealed that an equilibrium between complexes **[8]⁺** and **[11]⁺** was established in both cases and in order to reach completion it proved necessary to remove the solvent, and therefore the displaced acetonitrile, several times during the course of the reaction. Related osmium and ruthenium complexes have previously been prepared.²⁴

Complexes **[11a]PF₆** and **[11b]PF₆** were characterized by NMR spectroscopy and single crystal X-ray diffraction. The structure of **[11a]PF₆** is displayed in Figure 3 and demonstrates that the 2-styrylpyridine ligand is coordinated to the metal through both the nitrogen atom of the pyridine ring and the pendant alkene. The NMR spectra of complexes **[11a]⁺** and

Scheme 6^a



^a(i) CH₂Cl₂; (ii) + d₅-py.

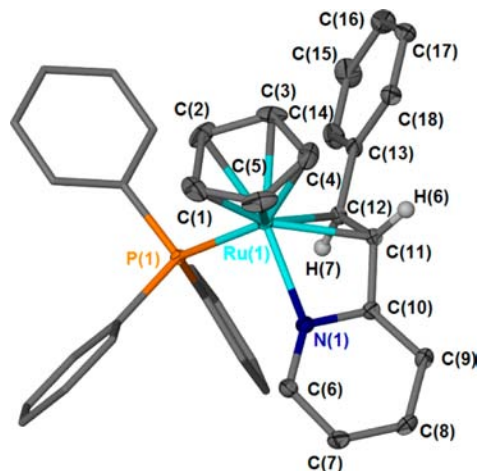
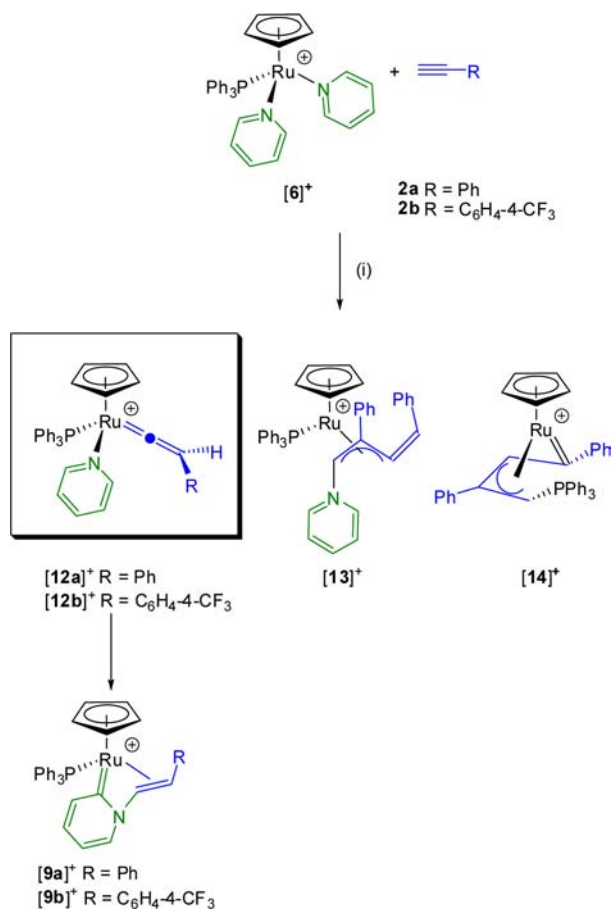


Figure 3. Solid-state structure of the cation **[11a]⁺**. Thermal ellipsoids (where shown) at the 50% probability level, hydrogen atoms (except H(11) and H(12)) omitted for clarity.

[11b]⁺ were temperature dependent. At 220 K, two isomeric forms of the complex were observed whereas at room temperature broad time-averaged signals were observed. The two interconverting isomers are thought to differ in the orientation of the alkene ligand relative to the [Ru(η^5 -C₅H₅)(PPh₃)] fragment (see Supporting Information).

Dissolution of [11a]PF₆ in d₅-pyridine resulted in the selective formation of the bis-pyridine complex [6]-d₁₀PF₆ and uncoordinated 2-styrylpyridine demonstrating that 7 is readily displaced from the ruthenium and product inhibition is unlikely. Therefore, the data are consistent with the formation of [10] being the primary deactivation route.

Mechanistic Investigations into the Formation of Pyridylidene Complexes. Treatment of a pyridine solution of [6]PF₆ with either 2a or 2b did not result in any reaction until heated to 50 °C, at which point the formation of 7a and 7b respectively was observed. In contrast, treatment of a room temperature CD₂Cl₂ solution of [6]PF₆ with one equivalent of H¹³C≡CPh, 2a-¹³C, resulted in the formation of three products (Scheme 7). The major product, [12a]⁺-¹³C, was

Scheme 7^a

^a(i) CH₂Cl₂.

identified as the vinylidene-containing complex [Ru(η^5 -C₅H₅)(py)(=CHPh)(PPh₃)]⁺ on the basis of the observation of a doublet resonance in the ¹³C{¹H} NMR spectrum at δ_C 355.2 (d, ²J_{PC} = 16.9 Hz); a corresponding doublet was observed in the ³¹P{¹H} NMR spectrum at δ_P 51.8. The ¹H NMR spectrum exhibited a broad resonance at δ_H 5.14 of relative integration one, due to the proton attached to the β -carbon of the

vinylidene ligand and a resonance with relative integration of two for the hydrogen atoms in the ortho-position of the coordinated pyridine at δ_H 8.40. A related compound, [Ru(η^5 -C₅H₅)(NCMe)(=C=CHSiMe₃)(PPh₃)]⁺, has been previously observed on reaction of [8]⁺ with HC≡CSiMe₃.²⁶ The observation of [12a]⁺-¹³C is an important one as this species was proposed by Murakami and Hori as a key intermediate on the route to 7a (Scheme 2b).¹⁸

The two minor products were shown to be complex [13]PF₆ and the known allyl-carbene complex [14]PF₆ previously reported by Kirchner (identified by comparison with an authentic sample).^{26,27} The identity of [13]PF₆ was confirmed by a single crystal X-ray diffraction study that demonstrated a condensation reaction between two molecules of the alkyne and a pyridine had occurred (Figure 4) to give an η^3 -coordinated butadienyl ligand.²⁸

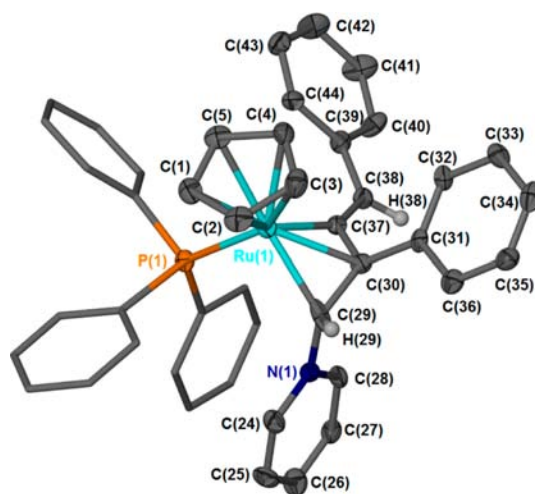


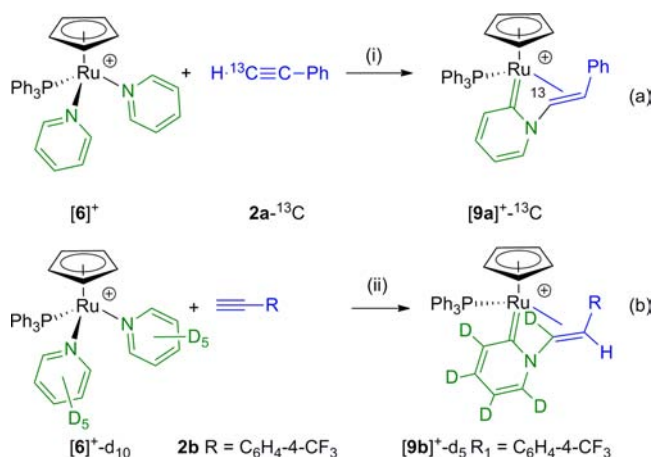
Figure 4. Solid-state structure of the cation [13]⁺. Thermal ellipsoids (where shown) are at the 50% probability level, and hydrogen atoms (except for H(29) and H(38)) were omitted for clarity.

Although [13]PF₆ proved to be only a minor component of the reaction mixture, further evidence for its formulation was obtained from the reaction between [6]PF₆ and H¹³C≡CPh. In this instance the resonance in the ³¹P{¹H} NMR spectrum assigned to [13]⁺-¹³C₂ was observed as a broad doublet-of-doublets (δ_P 48.1, ²J_{PC} = 12.2 and 6.3 Hz), consistent with the incorporation of two enriched alkynes into the product. Two isotopically enriched resonances were observed in the ¹³C{¹H} NMR spectrum due to [13]⁺-¹³C at δ_C 67.1 (d, ²J_{PC} = 7.7 Hz) and δ_C 170.8 (d, ²J_{PC} = 12.9 Hz) because of C(29) and C(37) respectively (Figure 4).

Related reactions between [6]⁺ and 2a or 2b in CD₂Cl₂ solution led to formation of [12a]⁺ and [12b]⁺ respectively. The reaction of [6]PF₆ with 2a in CD₂Cl₂ solution in the presence of two equivalents of pyridine resulted in the formation of [12a]PF₆ and [13]PF₆; no [14]PF₆ was observed. Increasing the quantity of alkyne in the reaction increased the proportion of [13]PF₆ produced. The most selective reaction was observed on treatment of [6]PF₆ with 2b in the presence of two equivalents of pyridine. In this instance, the only product observed in the initial reaction mixture was the vinylidene complex [12b]PF₆.

Complex [12]⁺ prepared in situ from the reaction between [6]PF₆ and 2a or 2b, converted slowly at room temperature in

CD_2Cl_2 solution to form the corresponding complex $[9]^+$. The $^{13}\text{C}\{^1\text{H}\}$ NMR spectrum of the product obtained from the reaction of $[6]\text{PF}_6$ with $2\text{-}^{13}\text{C}$ revealed that the resonance at δ_{C} 54.8 corresponded to an isotopically enriched carbon. The resonance in the ^1H NMR spectrum at δ_{H} 6.77 now exhibited an additional large coupling ($J_{\text{CH}} = 196$ Hz) whereas the resonance at δ_{H} 3.60 was unaffected. These data imply that the ^{13}C label has been incorporated at position C(11) (Figure 1, Scheme 8a). A ^1H NMR spectrum of the reaction of $[\text{Ru}(\eta^5-$

Scheme 8^a

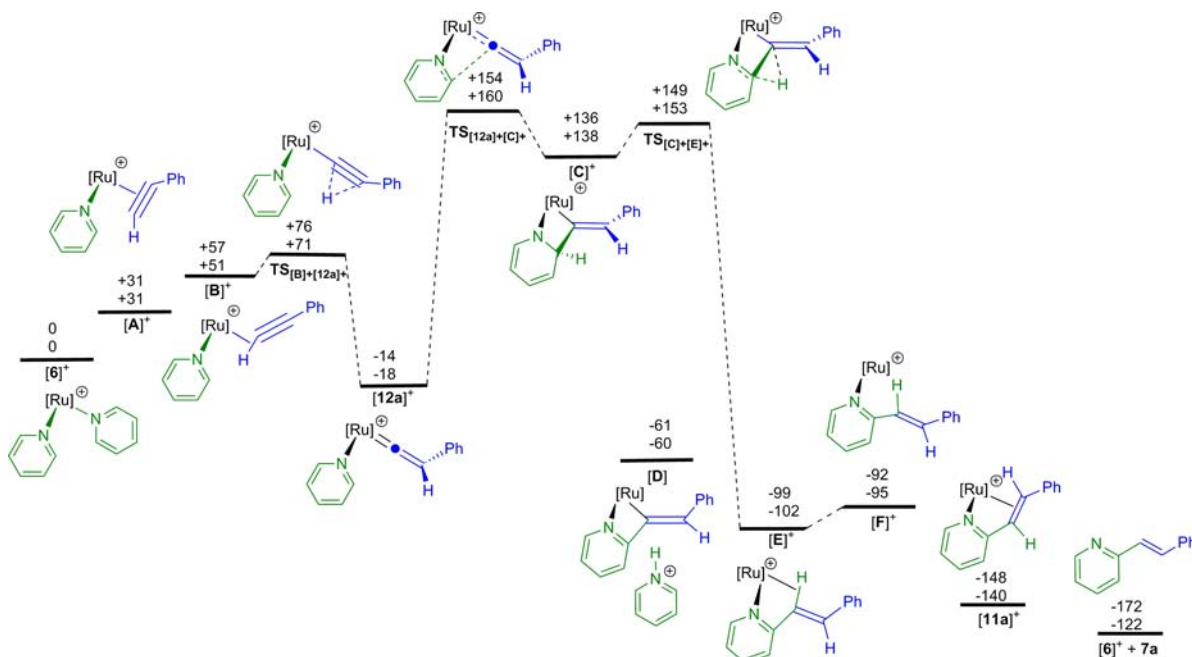
^a(i) CD_2Cl_2 , +2 py; (ii) CD_2Cl_2 , +2 d_5 -py.

$\text{C}_5\text{H}_5)(\text{NC}_5\text{D}_5)_2(\text{PPh}_3)]^+$, $[\text{6a}]^+ \cdot \text{-d}_{10}$ with 2a in the presence of NC_5D_5 revealed that the relative integration of the resonance at δ_{H} 3.60 (for H(12)) was unaffected but the peak at δ_{H} 6.77 was no longer observed, suggesting initial complete deuterium atom incorporation at this site. Although isotopic scrambling occurs

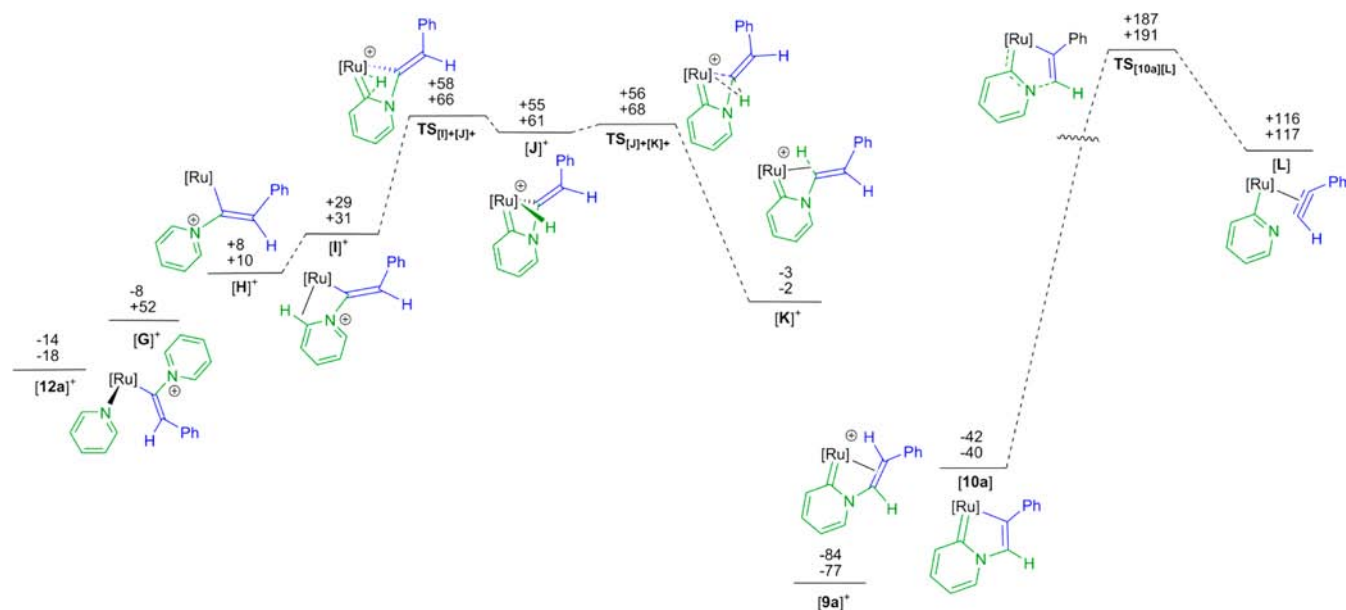
on prolonged standing, these data suggest that the H(12) was originally from the terminal alkyne (Scheme 8b). Both the ^{13}C and ^2H labeling studies are consistent with a vinylidene-containing complex acting as an intermediate in the formation of $[9]^+$.

The results from these synthetic and mechanistic studies indicate that $[6]^+$ may promote the formation of the desired 2-styrylpyridines, 7 and that the formation of the pyridylidene-containing complexes $[9]^+$ and $[10]$ represent catalyst deactivation. Furthermore, the vinylidene complex $[12]^+$ appears to be an important intermediate in the assembly of the pyridylidene ligands.

DFT Studies. A DFT study was undertaken to provide further insight into the key mechanistic processes underpinning the formation of the different organometallic and organic products observed in this study. Calculations were performed at the (RI-)PBE0/def2-TZVPP//((RI-)BP86/SV(P) level using the full ligand substituents employed in the experimental study.²⁹ Data presented below include pyridine solvation (using the COSMO method). Details of the gas phase and dichloromethane solvated data and other computational details are provided in the Supporting Information. ZPE-corrected SCF energies ($E_{\text{SCF}+\text{ZPE}}$) and Gibbs energies at 298.15 K (in kJ mol^{-1}) are both presented for the potential energy surfaces below and are quoted in relative to complex $[6]^+$. However, because of the difficulties associated with the assessment of Gibbs energies in solution, all energies discussed in the main text are $E_{\text{SCF}+\text{ZPE}}$.³⁰ Experimentally observed complexes are referred to by numbers, computationally generated structures are letters. Dotted lines on the PES indicate connectivity between minima and transition states (confirmed by DRC analysis). Steps, such as solvent-mediated deprotonation and ligand loss, are likely to be poorly modeled by the methodologies used, and as such, connections to neighboring states are not shown.

Scheme 9. Pathway A: Potential Energy Surface for the Formation of $[6]^+$ and 7a Based on the Mechanism Proposed by Murakami and Hori^{18a}

^a $[\text{Ru}] = [\text{Ru}(\eta^5\text{-C}_5\text{H}_5)(\text{PPh}_3)]$. Relative $E_{\text{SCF}+\text{ZPE}}$ (top) and Gibbs free energy (bottom) in pyridine (COSMO solvation) are shown in kJ mol^{-1} .

Scheme 10. Pathway B: Potential Energy Surface for the Formation of $[9a]^+$ from $[12a]^+$ ^a

^a[Ru] = [Ru(η^5 -C₅H₅)(PPh₃)]. Relative $E_{SCF+ZPE}$ (top) and Gibbs free energy (bottom) in pyridine (COSMO solvation) are shown in kJ mol⁻¹. Where appropriate, [Hpy]⁺ omitted for clarity.

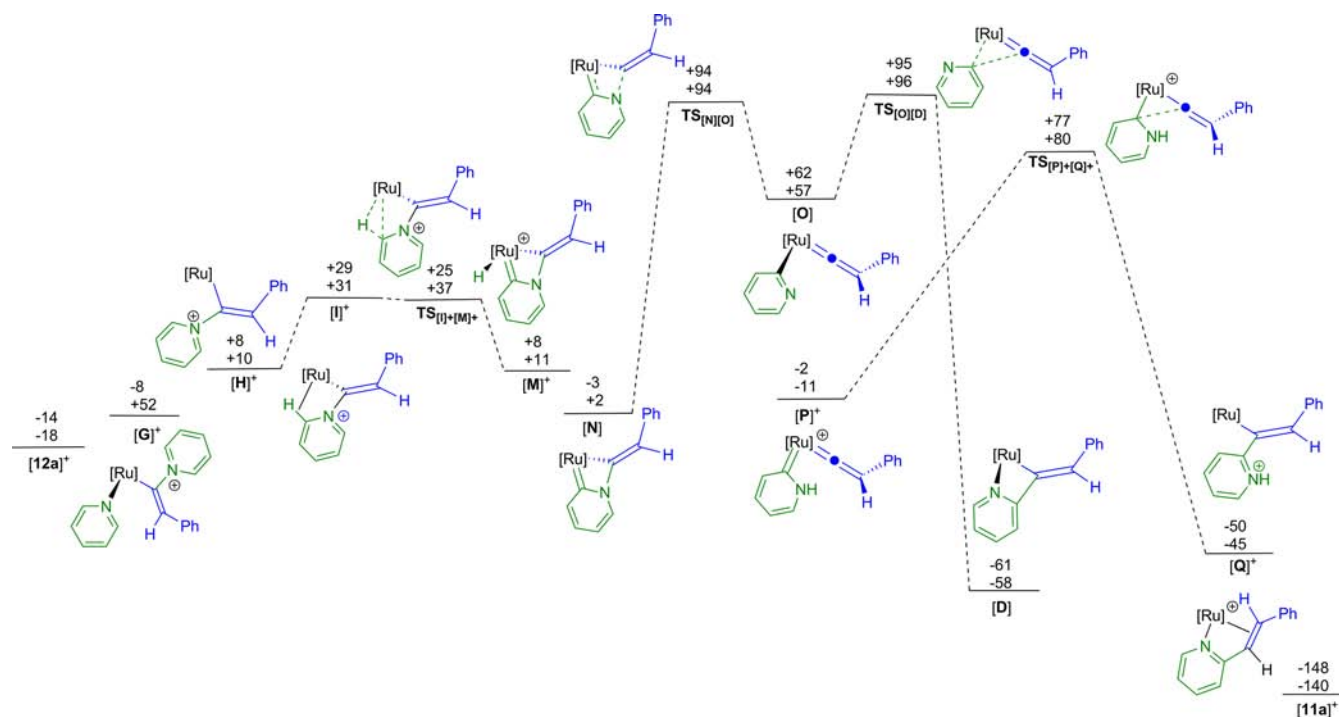
Given that the vinylidene complex $[12a]^+$ has been proposed by Murakami and Hori as a key intermediate in the formation of **7a** and that our experimental observations support this hypothesis, the formation and reactivity of this species were the starting point for the DFT study. The formation of $[12a]^+$ from $[6]^+$ is predicted to be energetically favorable ($\Delta E_{SCF+ZPE} = -14$ kJ mol⁻¹) and proceeds via a 1,2-hydrogen migration pathway (Scheme 9). The alkyne binds initially to the metal in an η^2 -fashion to give $[A]^+$, slippage to the related C–H σ -complex results in $[B]^+$. Hydrogen migration then occurs via $TS_{[B]+[12a]^+}$ to afford $[12a]^+$. This process is typical for PPh₃-containing half-sandwich ruthenium complexes.^{7b,h,31}

Three mechanistic pathways were then evaluated. In **Pathway A**, the formation of **7a** by the mechanism proposed by Murakami and Hori was probed. The formation of $[9a]^+$ is explored in **Pathway B**, and the generation of **7a** by an alternative pathway to that proposed by Murakami and Hori is described in **Pathway C**.

Pathway A involves a direct coupling between the α -carbon of the vinylidene ligand and carbon atom in the 2-position of the pyridine ring of $[12a]^+$ that may be viewed as an electrophilic substitution reaction. Our calculations reveal that the resulting intermediate $[C]^+$ lies at a relative energy of +136 kJ mol⁻¹ and is reached via the relatively high-energy transition state $TS_{[12a]+[C]^+}$ (+154 kJ mol⁻¹). Two pathways were then considered for the subsequent formation of the product. Simple deprotonation of $[C]^+$ by the pyridine solvent would afford $[D]$ (–61 kJ mol⁻¹), reprotonation at the metal-bound carbon of the alkenyl ligand then affords $[E]^+$ (–99 kJ mol⁻¹) which contains an agostic interaction between the α -C–H bond of the vinyl substituent. Cleavage of this agostic interaction, via $[F]^+$ allows access to $[11a]^+$ (–148 kJ mol⁻¹) and ultimately regenerate $[6]^+$ with concomitant formation of **7a** (–172 kJ mol⁻¹). An alternative pathway to $[E]^+$ involves a concerted hydrogen migration from pyridine to the alkenyl ligand via a high energy pathway involving $TS_{[C]+[E]^+}$ (+149 kJ mol⁻¹).

We have used the energetic span model of Kozuch and Shaik to compare the feasibilities of different mechanistic possibilities for these catalytic systems.³² **Pathway A** has a large energetic span of +168 kJ mol⁻¹ (where the TDI = $[12a]^+$ and the TDTS = $TS_{[12a]+[C]^+}$). This is not inconsistent with the relatively harsh reaction conditions used in Murakami and Hori's system (150 °C, 7 h). However, it does not explain the formation of product via our revised experimental conditions (50 °C, 2 d) described above. Also, a mechanistic proposal which accounts for both the formation of **7a** and the pyridylidene complex $[9a]^+$ is required. The electrophilic character of the metal-bound carbon atom of vinylidene ligands is well established, therefore **Pathway B** focuses on a mechanistic route involving nucleophilic attack by free pyridine at the α -carbon of the vinylidene in $[12a]^+$ (Scheme 10). This results in the formation of the alkenyl complex $[G]^+$, which on loss of the metal-bound pyridine affords $[H]^+$. The generation of a vacant coordination site allows for the formation of an intermediate agostic complex $[I]^+$, which exists as two key conformational isomers (see Supporting Information) each with a potentially different fate. In the first instance, C–H activation, via formal oxidative addition to the metal via $TS_{[I]+[J]^+}$ (+58 kJ mol⁻¹) affords the hydride complex $[J]^+$. Complex $[J]^+$ lies in a shallow minimum and it was necessary to fix the Ru–H bond during optimization to allow this state to be located.³³ Hydride migration via $TS_{[J]+[K]^+}$ then affords the agostic complex $[K]^+$, in which the alkenyl-pyridylidene ligand has been assembled. A shift from a C–H agostic interaction to η^2 -C=C binding modes then affords $[9a]^+$.

Pathway B is a relatively low energy process (energetic span for the formation of $[9a]^+ = +72$ kJ mol⁻¹; where TDI = $[12a]^+$ and TDTS = $TS_{[I]+[J]^+}$) compared to **Pathway A**, which proceeds via the high energy state $TS_{[12a]+[C]^+}$ (energetic span = +168 kJ mol⁻¹). This mechanistic possibility is consistent with the deuteration studies described above, as initial D incorporation from d₅-py into $[9a]^+$ would occur at the α -carbon of the vinyl group, as would be expected with an

Scheme 11. Pathway C: Potential Energy Surface for the Formation of $[11a]^+$ from $[12a]^{+\alpha}$ 

$^{\alpha}[\text{Ru}] = [\text{Ru}(\eta^5\text{-C}_5\text{H}_5)(\text{PPh}_3)_3]$. Relative $E_{\text{SCF}+\text{ZPE}}$ (top) and Gibbs free energy (bottom) in pyridine (COSMO solvation) are shown in kJ mol^{-1} . Where appropriate, $[\text{Hpy}]^+$ omitted for clarity.

intramolecular process. Complex $[9a]^+$ is calculated to be 84 kJ mol^{-1} lower in energy than the reference point and as such is a kinetic product of the reaction (the formation of **7a** and regeneration of $[6]^+$ represents the thermodynamic product in this system being energetically favorable by 172 kJ mol^{-1} compared to the reference point).

The calculations also indicate why $[10a]$ results in catalyst deactivation. The formation of the product from $[10a]$ may occur via two potential pathways, in the first instance, C–N bond cleavage may occur to give $[L]$. In principle $[L]$ could isomerize to $[O]$ which is a key intermediate in the formation of **7a** in Pathway C (q.v.). However, the transition state connecting $[10a]$ and $[L]$ ($\text{TS}_{[10a][L]}$) lies at very high energy ($+187 \text{ kJ mol}^{-1}$) leading to a large energetic span for this possibility ($+271 \text{ kJ mol}^{-1}$; where $\text{TDI} = [9a]^+$ and $\text{TDTS} = \text{TS}_{[10a][L]}$). Alternatively, $[10a]$ may revert to $[I]^+$ via $[9a]^+$, which then undergoes an alternative C–H bond activation, affording $[11a]^+$ (q.v.). However, the TDI for this process is now $[9a]^+$, which is significantly lower in energy than the vinylidene complex $[12a]^+$ leading to a large energetic span ($+179 \text{ kJ mol}^{-1}$; where $\text{TDI} = [9a]^+$ and $\text{TDTS} = \text{TS}_{[O][D]}$) for the formation of **7a** from $[9a]^+$, thus illustrating why the formation of the pyridylidene complex $[9a]^+$ and subsequent deprotonation to form $[10a]$ is a catalyst deactivation pathway.

Scheme 11 shows the alternative fate for $[I]^+$ as Pathway C, which involves oxidative addition of the C–H bond to the metal via transition state $\text{TS}_{[I][M]^+}$ (which is essentially isoenergetic with $[I]^+$ at this level of theory) to afford the pyridylidene-hydride complex $[M]^+$. Although $[M]^+$ (and $[J]^+$ encountered earlier) are formally hydrides, their partial charges ($+0.038$ for $[M]^+$ and $+0.085$ for $[J]^+$; from a PABOON population analysis) suggest protic rather than hydridic character. As such, deprotonation of $[M]^+$ by free pyridine can occur to give $[N]$ (alternatively, Pathway C may be

accessed at this point by deprotonation of $[J]^+$ to yield $[N]$, Scheme 10). Cleavage of the carbon–nitrogen bond via $\text{TS}_{[N][O]}$ ($+94 \text{ kJ mol}^{-1}$) results in the formation of pyridyl complex $[O]$ ($+62 \text{ kJ mol}^{-1}$). This is the microscopic reverse of the formation of related alkenyl complexes from a coordinated pyridyl ligand and vinylidene, which has been observed previously.^{8d} Pyridyl migration via $\text{TS}_{[O][D]}$ ($+95 \text{ kJ mol}^{-1}$) then affords $[D]$, which on protonation of the M–C bond yields $[11a]^+$ and subsequently liberation of **7a** with regeneration of $[6]^+$. The energetic span for the formation of **7a** from the catalyst $[6]^+$ via Pathway C is 109 kJ mol^{-1} (where $\text{TDI} = [12a]^+$ and $\text{TDTS} = \text{TS}_{[O][D]}$). This is significantly more favorable than formation of the product via the mechanism proposed by Murakami and Hori (energetic span = $+168 \text{ kJ mol}^{-1}$) or from the catalyst deactivation product $[10a]$ (energetic span = $+179 \text{ kJ mol}^{-1}$) and is consistent with the experimental conditions discussed above.

A further mechanistic possibility is that protonation of the nitrogen atom in the pyridyl ligand in $[O]$ will afford $[P]^+$ (-2 kJ mol^{-1}) generating a pyridylidene ligand. In this instance the transition state for C–C bond formation ($\text{TS}_{[P][Q]^+}$), which corresponds to pyridylidene migration to the vinylidene, is at a lower energy than the analogous transformation involving pyridyl migration ($\text{TS}_{[O][D]}$). Deprotonation of the product of pyridylidene migration, $[Q]^+$, may then result in the formation of $[D]$ which on subsequent reprotonation allows access to $[11a]^+$. Potential mechanisms for the isomerization of $[12a]^+$ to form $[P]^+$ are discussed in the Supporting Information.

Pathways B and C account for many of the experimental observations. For example, reactions performed in CH_2Cl_2 solution with only a small excess of pyridine result in the formation of $[9a]^+$. Presumably under these conditions, deprotonation of the intermediate pyridylidene-hydride complexes $[J]^+$ or $[M]^+$ is slow hence the kinetically preferred

product $[9a]^+$ is obtained. In contrast, when the reaction is performed under pyridine-rich conditions, the formation of the pyridylidene $[N]$ is promoted due to the excess of base and this pathway leads to the desired product **7a** occurs.

The proposed pathways also provide insight into the observed stereochemical outcome of the reaction. Both the formation of the metal-complex $[9a]^+$ and the final product **7a** proceeds in a highly selective manner to give the *E*-isomer of the alkene. The potential energy surface was surveyed for pathways leading to both the *E*-(*proE*-pathway) and *Z*-(*proZ*-pathway) isomers of the products. On the whole, most points were essentially isoenergetic, apart from the formally coordinatively unsaturated complexes $[H]^+$ and $[Q]^+$ (discussed in the Supporting Information) and the transition states $TS_{[N][O]}$ and $TS_{[O][D]}$. Importantly, the *proE*-isomer of $TS_{[O][D]}$, which is the TDTS for formation of **7a**, is 19 kJ mol⁻¹ lower in energy than the corresponding *proZ*-form. The origin of this energy difference appears to be an unfavorable steric clash between the phenyl ring of the alkenyl group and the pyridyl ligand in the *proZ*-isomer (Figure 5b): a similar

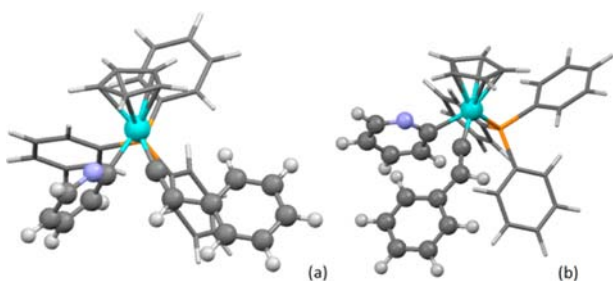
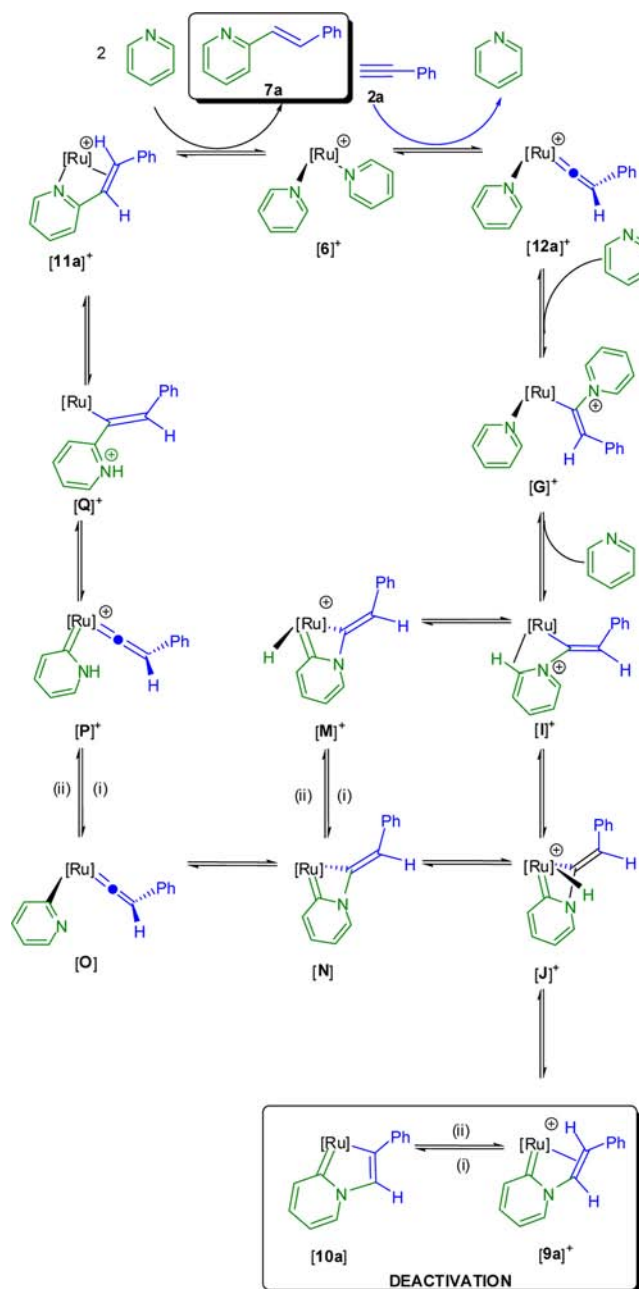


Figure 5. Structures of (a) *proE*- $TS_{[O][D]}$ and (b) *proZ*- $TS_{[O][D]}$.

clash is present in $TS_{[N][O]}$. This leads to an energetic span for formation of the *Z*-isomer of **7a** that is 25 kJ mol⁻¹ more positive and conveniently explains the stereoselectivity of the catalyst.

Proposed Catalytic Cycle. Experimental and theoretical data indicate that $[Ru(\eta^5-C_5H_5)(py)_2(PPh_3)]^+$, $[6]^+$, is the active species for the direct C–H functionalization of pyridine by terminal alkynes and a possible catalytic cycle is shown in Scheme 12. The first step of the reaction mechanism is the formation of the vinylidene complex $[Ru(\eta^5-C_5H_5)(py)(=C=CHR)(PPh_3)]^+$, $[12]^+$. The nitrogen atom in the pyridine acts as directing group toward the electrophilic α -carbon of the vinylidene ligand promoting formation of the σ -complex $[I]^+$. Complex $[I]^+$ may act as a precursor to the C–H activation products $[J]^+$ and $[M]^+$. A kinetically favored hydrogen-migration from $[J]^+$ occurs to give $[9]^+$. This is the dominant pathway observed in CH_2Cl_2 solution and results in catalyst deactivation. In contrast, for reactions performed in base-rich media (such as in pyridine solution) deprotonation of either intermediate metal pyridylidene-hydride may lead to productive catalysis. Access to $[N]$ allows for C–N bond cleavage before C–C bond formation by pyridylidene (or pyridyl) migration to the α -carbon of a Ru-vinylidene species from $[P]^+$. Therefore the generation of the pyridylidene/pyridyl ligand provides a lower energy pathway for C–C bond formation. Rearrangement of $[Q]^+$ followed by ligand substitution then affords **7**. Pyridine therefore plays two roles in the reaction: it acts as substrate and as an intermolecular proton shuttle deprotonating a hydride complex to promote the desired pathway to **7** and reprotonating either $[O]$ or $[D]$ to form the product.

Scheme 12^a



^a $[Ru] = [Ru(\eta^5-C_5H_5)(PPh_3)]$ (i) $-H^+$; (ii) $+H^+$.

CONCLUSIONS

On the basis of the mechanistic understanding gained from this study, we have demonstrated that the formation of 2-styrylpyridine from terminal alkynes and pyridine may be catalyzed by $[6]^+$. This occurs under far milder conditions than the corresponding reactions promoted by $[Ru(\eta^5-C_5H_5)Cl(PPh_3)_2]$. This entails that only trace amounts of dimerization of the terminal alkyne are observed indicating that the product may be formed with almost 100% atom efficiency and we are currently investigating the application of this methodology for the alkenylation of a range of N-heterocycles. Both the experimental and theoretical studies have demonstrated that pyridylidene ligands may play an important role in C–C bond formation reactions and thus are potentially attractive intermediates for the development of new C–H functionaliza-

tion reactions. Interestingly, in the system discussed here pyridylidene ligands are implicated in both productive and nonproductive mechanistic pathways.

The pyridylidene ligand in complex [9]⁺ appears to be formed via a different mechanism to those described for the related iridium^{8f} and rhodium-containing^{16a} systems. In these cases the first step in the reaction pathway is proposed to be the formation of a C–H σ -complex from the N-bound form of the heterocycle. In neither case is the carbene ligand formed directly from this intermediate. In the iridium case, a σ -CAM mechanism³⁴ occurs transferring a hydrogen first to a phenyl ligand then to the nitrogen atom of a pyridyl ligand. In the case of the rhodium system, formal oxidative addition of the C–H bond occurs via a σ -complex. A key feature of the current system is the templating by the vinylidene ligand. Nucleophilic attack by pyridine at the α -carbon of this ligand brings the C–H bond in the ortho position of the heterocycle into proximity of the metal hence promoting bond activation. An important consequence of this interaction is that pyridine is only activated in the 2-position hence the subsequent product is formed in a regioselective manner. Such mechanistic processes may provide an alternative to the existing directing groups employed in related direct C–H functionalization reactions. The development of the direct coupling of an unprotected terminal alkyne with pyridine and its derivatives provides a 100% atom efficient route to the catalytic functionalization of N-heterocycles, which may have significant synthetic applications.

■ ASSOCIATED CONTENT

■ Supporting Information

Detailed experimental procedures and characterization of compounds, details of the DFT calculations, including coordinates for all species investigated, and CIF with details of X-ray data collection and refinement for complexes [6]PF₆·CH₂Cl₂, [9a]PF₆·CH₂Cl₂, [9b]PF₆·CH₂Cl₂, [10b]·CH₂Cl₂, [11a]PF₆·CH₂Cl₂, [11b]PF₆·CH₂Cl₂, [13]PF₆·CH₂Cl₂. This material is available free of charge via the Internet at <http://pubs.acs.org>.

■ AUTHOR INFORMATION

Corresponding Author

jason.lynam@york.ac.uk; john.slattery@york.ac.uk

Notes

The authors declare no competing financial interest.

■ ACKNOWLEDGMENTS

We are grateful to the EPSRC (Grant EP/H011455/1) for funding this work. We are grateful to the U.K. National Crystallographic Service for the data collection of complex [13]PF₆·CH₂Cl₂. We are grateful to Professors Odile Eisenstein (Montpellier), Ian Fairlamb (York), and Robin Perutz (York) for insightful comments on this work.

■ REFERENCES

(1) (a) Bellina, F.; Rossi, R. *Chem. Rev.* **2010**, *110*, 1082–1146. (b) Doyle, M. P.; Duffy, R.; Ratnikov, M.; Zhou, L. *Chem. Rev.* **2010**, *110*, 704–724. (c) Mkhaliid, I. A. I.; Barnard, J. H.; Marder, T. B.; Murphy, J. M.; Hartwig, J. F. *Chem. Rev.* **2010**, *110*, 890–931. (d) Willis, M. C. *Chem. Rev.* **2010**, *110*, 725–748. (e) Gunay, A.; Theopold, K. H. *Chem. Rev.* **2010**, *110*, 1060–1081. (f) Boorman, T. C.; Larrosa, I. *Chem. Soc. Rev.* **2011**, *40*, 1910–1925. (g) Pitié, M.; Pratviel, G. v. *Chem. Rev.* **2010**, *110*, 1018–1059. (h) Sehnal, P.; Taylor, R. J. K.; Fairlamb, I. J. S. *Chem. Rev.* **2010**, *110*, 824–889.

(i) Balcells, D.; Clot, E.; Eisenstein, O. *Chem. Rev.* **2010**, *110*, 749–823. (j) Crabtree, R. H. *Chem. Rev.* **2010**, *110*, 575–575. (k) Che, C.-M.; Lo, V. K.-Y.; Zhou, C.-Y.; Huang, J.-S. *Chem. Soc. Rev.* **2011**, *40*, 1950–1975. (l) Davies, H. M. L.; Morton, D. *Chem. Soc. Rev.* **2011**, *40*, 1857–1869. (m) Collet, F.; Lescot, C.; Dauban, P. *Chem. Soc. Rev.* **2011**, *40*, 1926–1936. (n) Gutekunst, W. R.; Baran, P. S. *Chem. Soc. Rev.* **2011**, *40*, 1976–1991. (o) Lu, H.; Zhang, X. P. *Chem. Soc. Rev.* **2011**, *40*, 1899–1909. (p) Hartwig, J. F. *Chem. Soc. Rev.* **2011**, *40*, 1992–2002. (q) McMurray, L.; O'Hara, F.; Gaunt, M. J. *Chem. Soc. Rev.* **2011**, *40*, 1885–1898. (r) Zhang, S.-Y.; Zhang, F.-M.; Tu, Y.-Q. *Chem. Soc. Rev.* **2011**, *40*, 1937–1949. (s) Yeung, C. S.; Dong, V. M. *Chem. Rev.* **2011**, *111*, 1215–1292. (t) Engle, K. M.; Mei, T.-S.; Wasa, M.; Yu, J.-Q. *Acc. Chem. Res.* **2012**, *45*, 788–802. (u) Yamaguchi, J.; Yamaguchi, A. D.; Itami, K. *Angew. Chem., Int. Ed.* **2012**, *51*, 8960–9009. (v) Song, G.; Wang, F.; Li, X. *Chem. Soc. Rev.* **2012**, *41*, 3651–3678.

(2) Alberico, D.; Scott, M. E.; Lautens, M. *Chem. Rev.* **2007**, *107*, 174–238.

(3) (a) Kakiuchi, F.; Murai, S. *Acc. Chem. Res.* **2002**, *35*, 826–834. (b) Dupont, J.; Consorti, C. S.; Spencer, J. *Chem. Rev.* **2005**, *105*, 2527–2572. (c) Yu, J.-Q.; Giri, R.; Chen, X. *Org. Biomol. Chem.* **2006**, *4*, 4041–4047. (d) Seregin, I. V.; Gevorgyan, V. *Chem. Soc. Rev.* **2007**, *36*, 1173–1193. (e) Daugulis, O.; Do, H.-Q.; Shabashov, D. *Acc. Chem. Res.* **2009**, *42*, 1074–1086. (f) Jazzar, R.; Hitce, J.; Renaudat, A.; Sofack-Kreutzer, J.; Baudoin, O. *Chem.—Eur. J.* **2010**, *16*, 2654–2672. (g) Lyons, T. W.; Sanford, M. S. *Chem. Rev.* **2010**, *110*, 1147–1169. (h) Yeung, C. S.; Zhao, X.; Borduas, N.; Dong, V. M. *Chem. Soc. Rev.* **2010**, *1*, 331–336. (i) Zhao, X.; Yeung, C. S.; Dong, V. M. *J. Am. Chem. Soc.* **2010**, *132*, 5837–5844. (j) Lee, P.-S.; Fujita, T.; Yoshikai, N. *J. Am. Chem. Soc.* **2011**, *133*, 17283–17295. (k) Li, D.-D.; Yuan, T.-T.; Wang, G.-W. *Chem. Commun.* **2011**, *47*, 12789–12791. (l) Romero-Revilla, J. A.; García-Rubia, A.; Gómez Arrayás, R.; Fernández-Ibáñez, M. Á.; Carretero, J. C. *J. Org. Chem.* **2011**, *76*, 9525–9530. (m) Tredwell, M. J.; Gulias, M.; Bremeyer, N. G.; Johansson, C. C.; Collins, B. S.; Gaunt, M. J. *Angew. Chem., Int. Ed.* **2011**, *50*, 1076–1079. (n) Wencel-Delord, J.; Droge, T.; Liu, F.; Glorius, F. *Chem. Soc. Rev.* **2011**, *40*, 4740–4761.

(4) (a) Davies, D. L.; Donald, S. M. A.; Macgregor, S. A. *J. Am. Chem. Soc.* **2005**, *127*, 13754–13755. (b) Lafrance, M.; Rowley, C. N.; Woo, T. K.; Fagnou, K. J. *Am. Chem. Soc.* **2006**, *128*, 8754–8756. (c) Özdemir, I.; Demir, S.; Çetinkaya, B.; Gourlaouen, C.; Maseras, F.; Bruneau, C.; Dixneuf, P. H. *J. Am. Chem. Soc.* **2008**, *130*, 1156–1157. (d) Boutadla, Y.; Davies, D. L.; Macgregor, S. A.; Poblador-Bahamonde, A. I. *Dalton Trans.* **2009**, 5820–5831. (e) Pozgan, F.; Dixneuf, P. H. *Adv. Synth. Catal.* **2009**, *351*, 1737–1743. (f) Ackermann, L.; Novak, P.; Vicente, R.; Pirovano, V.; Potukuchi, H. K. *Synthesis* **2010**, 2245–2253. (g) Ackermann, L.; Vicente, R.; Potukuchi, H. K.; Pirovano, V. *Org. Lett.* **2010**, *12*, 5032–5035. (h) Arockiam, P. B.; Fischmeister, C.; Bruneau, C.; Dixneuf, P. H. *Angew. Chem., Int. Ed.* **2010**, *49*, 6629–6632. (i) Kefalidis, C. E.; Baudoin, O.; Clot, E. *Dalton Trans.* **2010**, *39*, 10528–10535. (j) Ackermann, L. *Chem. Rev.* **2011**, *111*, 1315–1345. (k) Ackermann, L.; Fenner, S. *Org. Lett.* **2011**, *13*, 6548–6551. (l) Ackermann, L.; Hofmann, N.; Vicente, R. *Org. Lett.* **2011**, *13*, 1875–1877. (m) Ackermann, L.; Lygin, A. V. *Org. Lett.* **2011**, *13*, 3332–3335. (n) Ackermann, L.; Lygin, A. V.; Hofmann, N. *Org. Lett.* **2011**, *13*, 3278–3281. (o) Ackermann, L.; Lygin, A. V.; Hofmann, N. *Angew. Chem., Int. Ed.* **2011**, *50*, 6379–6382. (p) Ackermann, L.; Pospech, J. *Org. Lett.* **2011**, *13*, 4153–4155. (q) Arockiam, P. B.; Fischmeister, C.; Bruneau, C.; Dixneuf, P. H. *Green Chem.* **2011**, *13*, 3075–3078. (r) Ferrer Flegeau, E.; Bruneau, C.; Dixneuf, P. H.; Jutand, A. *J. Am. Chem. Soc.* **2011**, *133*, 10161–10170. (s) Li, B.; Bheeter, C. B.; Darcel, C.; Dixneuf, P. H. *ACS Catal.* **2011**, *1*, 1221–1224. (t) Li, W.; Arockiam, P. B.; Fischmeister, C.; Bruneau, C.; Dixneuf, P. H. *Green Chem.* **2011**, *13*, 2315–2319. (u) Ackermann, L.; Diers, E.; Manvar, A. *Org. Lett.* **2012**, *14*, 1154–1157. (v) Ackermann, L.; Lygin, A. V. *Org. Lett.* **2012**, *14*, 764–767. (w) Ackermann, L.; Pospech, J.; Graczyk, K.; Rauch, K. *Org. Lett.* **2012**, *14*, 930–933. (x) Ackermann, L.; Wang, L.; Wolfram, R.; Lygin, A. V. *Org. Lett.* **2012**, *14*, 728–731.

(5) Kunz, D. *Angew. Chem., Int. Ed.* **2007**, *46*, 3405–3408.

- (6) (a) Lavorato, D.; Terlouw, J. K.; Dargel, T. K.; Koch, W.; McGibbon, G. A.; Schwarz, H. *J. Am. Chem. Soc.* **1996**, *118*, 11898–11904. (b) Lavorato, D. J.; Terlouw, J. K.; McGibbon, G. A.; Dargel, T. K.; Koch, W.; Schwarz, H. *Int. J. Mass Spectrom.* **1998**, *180*, 7–14.
- (7) (a) Bruce, M. I. *Chem. Rev.* **1991**, *91*, 197–257. (b) Wakatsuki, Y. *J. Organomet. Chem.* **2004**, *689*, 4092–4109. (c) Grotjahn, D. B.; Zeng, X.; Cooksy, A. L. *J. Am. Chem. Soc.* **2006**, *128*, 2798–2799. (d) De Angelis, F.; Sgamellotti, A.; Re, N. *Organometallics* **2007**, *26*, 5285–5288. (e) Cowley, M. J.; Lynam, J. M.; Slattery, J. M. *Dalton Trans.* **2008**, 4552–4554. (f) Vastine, B. A.; Hall, M. B. *Organometallics* **2008**, *27*, 4325–4333. (g) Johnson, D. G.; Lynam, J. M.; Slattery, J. M.; Welby, C. E. *Dalton Trans.* **2010**, *39*, 10432–10441. (h) Lynam, J. M. *Chem.—Eur. J.* **2010**, *16*, 8238–8247.
- (8) (a) Alvarez, E.; Conejero, S.; Paneque, M.; Petronilho, A.; Poveda, M. L.; Serrano, O.; Carmona, E. *J. Am. Chem. Soc.* **2006**, *128*, 13060–13061. (b) Álvarez, E.; Conejero, S.; Lara, P.; López, J. A.; Paneque, M.; Petronilho, A.; Poveda, M. L.; del Río, D.; Serrano, O.; Carmona, E. *J. Am. Chem. Soc.* **2007**, *129*, 14130–14131. (c) Conejero, S.; Lara, P.; Paneque, M.; Petronilho, A.; Poveda, M. L.; Serrano, O.; Vattier, F.; Alvarez, E.; Maya, C.; Salazar, V.; Carmona, E. *Angew. Chem., Int. Ed.* **2008**, *47*, 4380–4383. (d) Álvarez, E.; Hernández, Y. A.; López-Serrano, J.; Maya, C.; Paneque, M.; Petronilho, A.; Poveda, M. L.; Salazar, V.; Vattier, F.; Carmona, E. *Angew. Chem., Int. Ed.* **2010**, *49*, 3496–3499. (e) Hernández, Y. A.; López-Serrano, J.; Paneque, M.; Poveda, M. L.; Vattier, F.; Salazar, V.; Álvarez, E.; Carmona, E. *Chem.—Eur. J.* **2011**, *17*, 9302–9305. (f) Conejero, S.; López-Serrano, J.; Paneque, M.; Petronilho, A.; Poveda, M. L.; Vattier, F.; Álvarez, E.; Carmona, E. *Chem.—Eur. J.* **2012**, *18*, 4644–4664.
- (9) (a) Esteruelas, M. A.; Fernández-Alvarez, F. J.; Oñate, E. *J. Am. Chem. Soc.* **2006**, *128*, 13044–13045. (b) Esteruelas, M. A.; Fernández-Alvarez, F. J.; Oñate, E. *Organometallics* **2007**, *26*, 5239–5245. (c) Eguillor, B.; Esteruelas, M. A.; Oliván, M.; Puerta, M. *Organometallics* **2008**, *27*, 445–450. (d) Esteruelas, M. A.; Fernández-Alvarez, F. J.; Oñate, E. *Organometallics* **2008**, *27*, 6236–6244. (e) Esteruelas, M. A.; Fernández-Alvarez, F. J.; Oliván, M.; Oñate, E. *Organometallics* **2009**, *28*, 2276–2284.
- (10) Brill, M.; Díaz, J.; Huertos, M. A.; López, R.; Pérez, J.; Riera, L. *Chem.—Eur. J.* **2011**, *17*, 8584–8595.
- (11) (a) Ruiz, J.; Perandones, B. F. *J. Am. Chem. Soc.* **2007**, *129*, 9298–9299. (b) Ruiz, J.; Perandones, B. F.; Van der Maelen, J. F.; García-Granda, S. *Organometallics* **2010**, *29*, 4639–4642.
- (12) Huertos, M. A.; Pérez, J.; Riera, L.; Menéndez-Veldazquez, A. J. *Am. Chem. Soc.* **2008**, *130*, 13530–13531.
- (13) Burling, S. J.; Mahon, M. F.; Powell, R. E.; Whittlesey, M. K.; Williams, J. M. J. *J. Am. Chem. Soc.* **2006**, *128*, 13702–13703.
- (14) (a) Trost, B. M.; Frederiksen, M. U.; Rudd, M. T. *Angew. Chem., Int. Ed.* **2005**, *44*, 6630–6666. (b) Bruneau, C.; Dixneuf, P. H. *Angew. Chem., Int. Ed.* **2006**, *45*, 2176–2203. (c) Trost, B. M.; McClory, A. *Chem.—Asian J.* **2008**, *3*, 164–194.
- (15) (a) Berman, A. M.; Bergman, R. G.; Ellman, J. A. *J. Org. Chem.* **2010**, *75*, 7863–7868. (b) Lewis, J. C.; Bergman, R. G.; Ellman, J. A. *J. Am. Chem. Soc.* **2007**, *129*, 5332–5333. (c) Berman, A. M.; Lewis, J. C.; Bergman, R. G.; Ellman, J. A. *J. Am. Chem. Soc.* **2008**, *130*, 14926–14927.
- (16) (a) Wiedemann, S. H.; Lewis, J. C.; Ellman, J. A.; Bergman, R. G. *J. Am. Chem. Soc.* **2006**, *128*, 2452–2462. (b) Lewis, J. C.; Bergman, R. G.; Ellman, J. A. *Acc. Chem. Res.* **2008**, *41*, 1013–1025. (c) Colby, D. A.; Bergman, R. G.; Ellman, J. A. *Chem. Rev.* **2010**, *110*, 624–655. (d) Yotphan, S.; Bergman, R. G.; Ellman, J. A. *Org. Lett.* **2010**, *12*, 2978–2981. (e) Colby, D. A.; Tsai, A. S.; Bergman, R. G.; Ellman, J. A. *Acc. Chem. Res.* **2012**, *45*, 814–825.
- (17) Tan, K. L.; Bergman, R. G.; Ellman, J. A. *J. Am. Chem. Soc.* **2002**, *124*, 3202–3203.
- (18) Murakami, M.; Hori, S. *J. Am. Chem. Soc.* **2003**, *125*, 4720–4721.
- (19) Bruce, M. I.; Wallis, R. C. *Aust. J. Chem.* **1979**, *32*, 1471–1485.
- (20) (a) Bianchini, C.; Casares, J. A.; Peruzzini, M.; Romerosa, A.; Zanobini, F. *J. Am. Chem. Soc.* **1996**, *118*, 4585–4594. (b) Bianchini, C.; Innocenti, P.; Peruzzini, M.; Romerosa, A.; Zanobini, F. *Organometallics* **1996**, *15*, 272–285. (c) Hiett, N. P.; Lynam, J. M.; Welby, C. E.; Whitwood, A. C. *J. Organomet. Chem.* **2011**, *696*, 378–387.
- (21) Rüba, E.; Simanko, W.; Mauthner, K.; Soldouzi, K. M.; Slugovc, C.; Mereiter, K.; Schmid, R.; Kirchner, K. *Organometallics* **1999**, *18*, 3843–3850.
- (22) (a) Bianchini, C.; Peruzzini, M.; Zanobini, F.; Frediani, P.; Albinati, A. *J. Am. Chem. Soc.* **1991**, *113*, 5453–5454. (b) Bianchini, C.; Frediani, P.; Masi, D.; Peruzzini, M.; Zanobini, F. *Organometallics* **1994**, *13*, 4616–4632. (c) Slugovc, C.; Mereiter, K.; Zobetz, E.; Schmid, R.; Kirchner, K. *Organometallics* **1996**, *15*, 5275–5277. (d) Yi, C. S.; Liu, N. H. *Organometallics* **1996**, *15*, 3968–3971. (e) Yi, C. S.; Liu, N. H.; Rheingold, A. L.; Liable-Sands, L. M. *Organometallics* **1997**, *16*, 3910–3913. (f) Bassetti, M.; Marini, S.; Díaz, J.; Gamasa, M. P.; Gimeno, J.; Rodríguez-Álvarez, Y.; García-Granda, S. *Organometallics* **2002**, *21*, 4815–4822. (g) Chen, X. G.; Xue, P.; Sung, H. H. Y.; Williams, I. D.; Peruzzini, M.; Bianchini, C.; Jia, G. C. *Organometallics* **2005**, *24*, 4330–4332. (h) Dingwall, L. D.; Corcoran, C. M.; Lee, A. F.; Olivi, L.; Lynam, J. M.; Wilson, K. *Catal. Commun.* **2008**, *10*, 53–56. (i) Hijazi, A.; Parkhomenko, K.; Djukic, J.-P.; Chemmi, A.; Pfeiffer, M. *Adv. Synth. Catal.* **2008**, *350*, 1493–1496. (j) Lee, J.-H.; Caulton, K. G. *J. Organomet. Chem.* **2008**, *693*, 1664–1673. (k) Lynam, J. M.; Nixon, T. D.; Whitwood, A. C. *J. Organomet. Chem.* **2008**, *693*, 3103–3110. (l) Pasquini, C.; Bassetti, M. *Adv. Synth. Catal.* **2010**, *352*, 2405–2410. (m) Coniglio, A.; Bassetti, M.; García-Garrido, S. E.; Gimeno, J. *Adv. Synth. Catal.* **2012**, *354*, 148–158.
- (23) Cowley, M. J.; Lynam, J. M.; Moneyppenny, R. S.; Whitwood, A. C.; Wilson, A. J. *Dalton Trans.* **2009**, 9529–9542.
- (24) Castro-Rodrigo, R.; Esteruelas, M. A.; Fuertes, S.; López, A. M.; Mozo, S.; Oñate, E. *Organometallics* **2009**, *28*, 5941–5951.
- (25) (a) Foley, N. A.; Lail, M.; Gunnoe, T. B.; Cundari, T. R.; Boyle, P. D.; Petersen, J. L. *Organometallics* **2007**, *26*, 5507–5516. (b) Foley, N. A.; Lail, M.; Lee, J. P.; Gunnoe, T. B.; Cundari, T. R.; Petersen, J. L. *J. Am. Chem. Soc.* **2007**, *129*, 6765–6781. (c) Feng, Y.; Lail, M.; Foley, N. A.; Gunnoe, T. B.; Barakat, K. A.; Cundari, T. R.; Petersen, J. L. *J. Am. Chem. Soc.* **2006**, *128*, 7982–7994. (d) Chang, J.; Seidler, M. D.; Bergman, R. G. *J. Am. Chem. Soc.* **1989**, *111*, 3258–3271. (e) Diversi, P.; Fuligni, M.; Marchetti, F.; Pinzino, C. *J. Organomet. Chem.* **2005**, *690*, 605–612. (f) Boncella, J. M.; Eve, T. M.; Rickman, B.; Abboud, K. A. *Polyhedron* **1998**, *17*, 725–736. (g) Lehmkuhl, H.; Schwickardi, R.; Mehler, G.; Krüger, C.; Goddard, R. Z. *Anorg. Allg. Chem.* **1991**, *606*, 141–155. (h) Moss, J. R.; Ngubane, S.; Sivaramakrishna, A.; Makhubela, B. C. E.; Bercaw, J. E.; Labinger, J. A.; Day, M. W.; Henling, L. M.; Su, H. *J. Organomet. Chem.* **2008**, *693*, 2700–2702. (i) Burns, R. M.; Hubbard, J. L. *J. Am. Chem. Soc.* **1994**, *116*, 9514–9520. (j) Attar, S.; Catalano, V. J.; Nelson, J. H. *Syn. React. Inorg. Met.* **1998**, *28*, 749–755.
- (26) Rüba, E.; Mereiter, K.; Schmid, R.; Sapunov, V. N.; Kirchner, K.; Schottenberger, H.; Calhorda, M. J.; Veiros, L. F. *Chem.—Eur. J.* **2002**, *8*, 3948–3961.
- (27) Mauthner, K.; Soldouzi, K. M.; Mereiter, K.; Schmid, R.; Kirchner, K. *Organometallics* **1999**, *18*, 4681–4683.
- (28) (a) Bruce, M. I.; Rodgers, J. R.; Snow, M. R.; Swincer, A. G. *J. Chem. Soc., Chem. Commun.* **1981**, 271–272. (b) Brisdon, B. J.; Deeth, R. J.; Hodson, A. G. W.; Kemp, C. M.; Mahon, M. F.; Molloy, K. C. *Organometallics* **1991**, *10*, 1107–1115. (c) Benyunes, S. A.; Deeth, R. J.; Fries, A.; Green, M.; McPartlin, M.; Nation, C. B. M. *J. Chem. Soc., Dalton Trans.* **1992**, 3453–3465. (d) Brisdon, B. J.; Walton, R. A. *Polyhedron* **1995**, *14*, 1259–1276. (e) Yi, C. S.; Liu, N.; Rheingold, A. L.; Liable-Sands, L. M. *Organometallics* **1997**, *16*, 3910–3913. (f) Hodson, A. G. W.; Thind, R. K.; Granville-George, O. *J. Organomet. Chem.* **2004**, *689*, 2114–2122. (g) Bruce, M. I.; Fox, M. A.; Low, P. J.; Skelton, B. W.; Zaitseva, N. N. *Dalton Trans.* **2010**, 3759–3770. (h) Krivykh, V. V.; Glukhov, I. V. *Mendeleev Commun.* **2010**, *20*, 177–179. (i) Bruce, M. I. *Aust. J. Chem.* **2011**, *64*, 77–103. (j) Zhang, W.-Q.; Atkin, A. J.; Fairlamb, I. J. S.; Whitwood, A. C.; Lynam, J. M. *Organometallics* **2011**, *30*, 4643–4654.
- (29) (a) Pulay, P. *Chem. Phys. Lett.* **1980**, *23*, 393–398. (b) Császár, P.; Pulay, P. *J. Mol. Struct.* **1984**, *114*, 31–34. (c) Koga, T.; Kobayashi,

- H. *J. Chem. Phys.* **1985**, *82*, 1437–1439. (d) Ahlrichs, R.; Bär, M.; Häser, M.; Horn, H.; Kölmel, C. *Chem. Phys. Lett.* **1989**, *162*, 165–169. (e) Eichkorn, K.; Treutler, O.; Öhm, H.; Haeser, M.; Ahlrichs, R. *Chem. Phys. Lett.* **1995**, *240*, 283–290. (f) Treutler, O.; Ahlrichs, R. *J. Chem. Phys.* **1995**, *102*, 346–354. (g) Eichkorn, K.; Weigend, F.; Treutler, O.; Ahlrichs, R. *Theor. Chem. Acc.* **1997**, *97*, 119–124. (h) Arnim, M. v.; Ahlrichs, R. *J. Chem. Phys.* **1999**, *111*, 9183–9190. (i) Deglmann, P.; Furche, F. *J. Chem. Phys.* **2002**, *117*, 9535–9538. (j) Weigend, F. *Phys. Chem. Chem. Phys.* **2006**, *8*, 1057–1065.
- (30) (a) Leung, B. O.; Reid, D. L.; Armstrong, D. A.; Rauk, A. *J. Phys. Chem. A* **2004**, *108*, 2720–2725. (b) Ardura, D.; López, R.; Sordo, T. L. *J. Phys. Chem. B* **2005**, *109*, 23618–23623. (c) Dub, P. A.; Poli, R. *J. Mol. Cat. A* **2010**, *324*, 89–96.
- (31) De Angelis, F.; Sgamellotti, A.; Re, N. *Organometallics* **2002**, *21*, 5944–5950.
- (32) Kozuch, S.; Shaik, S. *Acc. Chem. Res.* **2010**, *44*, 101–110.
- (33) Attempts to locate this minimum using a range of optimization parameters failed, with “free” optimizations always proceeding to $[K]^+$. DRC runs from $TS_{[J][K]^+}$ suggest the presence of a stationary point on the PES close to $[J]^+$.
- (34) Perutz, R. N.; Sabo-Etienne, S. *Angew. Chem., Int. Ed.* **2007**, *46*, 2578–2592.

■ NOTE ADDED IN PROOF

Subsequent to the submission of our manuscript, Esteruelas and co-workers have demonstrated that an osmium vinylidene may undergo carbon–carbon bond formation with a pyridylidene-derived ligand. This process corresponds to the conversation of $[O]$ to $[D]$ (Scheme 11) in our study. See Bajo, S.; Esteruelas, M. A.; López, A. M.; Oñate, E. *Organometallics* **2012**, *31*, 8618–8626.